

## Measurement of the $B^0$ Meson Lifetime with Partial Reconstruction of $B^0 \rightarrow D^{*-}\pi^+$ and $B^0 \rightarrow D^{*-}\rho^+$ Decays

B. Aubert,<sup>1</sup> R. Barate,<sup>1</sup> D. Boutigny,<sup>1</sup> J.-M. Gaillard,<sup>1</sup> A. Hicheur,<sup>1</sup> Y. Karyotakis,<sup>1</sup> J. P. Lees,<sup>1</sup> P. Robbe,<sup>1</sup> V. Tisserand,<sup>1</sup> A. Zghiche,<sup>1</sup> A. Palano,<sup>2</sup> A. Pompili,<sup>2</sup> J. C. Chen,<sup>3</sup> N. D. Qi,<sup>3</sup> G. Rong,<sup>3</sup> P. Wang,<sup>3</sup> Y. S. Zhu,<sup>3</sup> G. Eigen,<sup>4</sup> I. Ofte,<sup>4</sup> B. Stugu,<sup>4</sup> G. S. Abrams,<sup>5</sup> A. W. Borgland,<sup>5</sup> A. B. Breon,<sup>5</sup> D. N. Brown,<sup>5</sup> J. Button-Shafer,<sup>5</sup> R. N. Cahn,<sup>5</sup> E. Charles,<sup>5</sup> M. S. Gill,<sup>5</sup> A. V. Gritsan,<sup>5</sup> Y. Groysman,<sup>5</sup> R. G. Jacobsen,<sup>5</sup> R. W. Kadel,<sup>5</sup> J. Kadyk,<sup>5</sup> L. T. Kerth,<sup>5</sup> Yu. G. Kolomensky,<sup>5</sup> J. F. Kral,<sup>5</sup> C. LeClerc,<sup>5</sup> M. E. Levi,<sup>5</sup> G. Lynch,<sup>5</sup> L. M. Mir,<sup>5</sup> P. J. Oddone,<sup>5</sup> T. J. Orimoto,<sup>5</sup> M. Pripstein,<sup>5</sup> N. A. Roe,<sup>5</sup> A. Romosan,<sup>5</sup> M. T. Ronan,<sup>5</sup> V. G. Shelkov,<sup>5</sup> A. V. Telnov,<sup>5</sup> W. A. Wenzel,<sup>5</sup> T. J. Harrison,<sup>6</sup> C. M. Hawkes,<sup>6</sup> D. J. Knowles,<sup>6</sup> S. W. O'Neale,<sup>6</sup> R. C. Penny,<sup>6</sup> A. T. Watson,<sup>6</sup> N. K. Watson,<sup>6</sup> T. Deppermann,<sup>7</sup> K. Goetzen,<sup>7</sup> H. Koch,<sup>7</sup> B. Lewandowski,<sup>7</sup> M. Pelizaeus,<sup>7</sup> K. Peters,<sup>7</sup> H. Schmuecker,<sup>7</sup> M. Steinke,<sup>7</sup> N. R. Barlow,<sup>8</sup> W. Bhimji,<sup>8</sup> J. T. Boyd,<sup>8</sup> N. Chevalier,<sup>8</sup> P. J. Clark,<sup>8</sup> W. N. Cottingham,<sup>8</sup> C. Mackay,<sup>8</sup> F. F. Wilson,<sup>8</sup> C. Hearty,<sup>9</sup> T. S. Mattison,<sup>9</sup> J. A. McKenna,<sup>9</sup> D. Thiessen,<sup>9</sup> S. Jolly,<sup>10</sup> P. Kyberd,<sup>10</sup> A. K. McKemey,<sup>10</sup> V. E. Blinov,<sup>11</sup> A. D. Bukin,<sup>11</sup> A. R. Buzykaev,<sup>11</sup> V. B. Golubev,<sup>11</sup> V. N. Ivanchenko,<sup>11</sup> A. A. Korol,<sup>11</sup> E. A. Kravchenko,<sup>11</sup> A. P. Onuchin,<sup>11</sup> S. I. Serednyakov,<sup>11</sup> Yu. I. Skovpen,<sup>11</sup> A. N. Yushkov,<sup>11</sup> D. Best,<sup>12</sup> M. Chao,<sup>12</sup> D. Kirkby,<sup>12</sup> A. J. Lankford,<sup>12</sup> M. Mandelkern,<sup>12</sup> S. McMahon,<sup>12</sup> R. K. Mommsen,<sup>12</sup> D. P. Stoker,<sup>12</sup> C. Buchanan,<sup>13</sup> H. K. Hadavand,<sup>14</sup> E. J. Hill,<sup>14</sup> D. B. MacFarlane,<sup>14</sup> H. P. Paar,<sup>14</sup> Sh. Rahatlou,<sup>14</sup> G. Raven,<sup>14</sup> U. Schwanke,<sup>14</sup> V. Sharma,<sup>14</sup> J. W. Berryhill,<sup>15</sup> C. Campagnari,<sup>15</sup> B. Dahmes,<sup>15</sup> N. Kuznetsova,<sup>15</sup> S. L. Levy,<sup>15</sup> O. Long,<sup>15</sup> A. Lu,<sup>15</sup> M. A. Mazur,<sup>15</sup> J. D. Richman,<sup>15</sup> W. Verkerke,<sup>15</sup> J. Beringer,<sup>16</sup> A. M. Eisner,<sup>16</sup> M. Grothe,<sup>16</sup> C. A. Heusch,<sup>16</sup> W. S. Lockman,<sup>16</sup> T. Pulliam,<sup>16</sup> T. Schalk,<sup>16</sup> R. E. Schmitz,<sup>16</sup> B. A. Schumm,<sup>16</sup> A. Seiden,<sup>16</sup> M. Turri,<sup>16</sup> W. Walkowiak,<sup>16</sup> D. C. Williams,<sup>16</sup> M. G. Wilson,<sup>16</sup> J. Albert,<sup>17</sup> E. Chen,<sup>17</sup> G. P. Dubois-Felsmann,<sup>17</sup> A. Dvoretzki,<sup>17</sup> D. G. Hitlin,<sup>17</sup> I. Narsky,<sup>17</sup> F. C. Porter,<sup>17</sup> A. Ryd,<sup>17</sup> A. Samuel,<sup>17</sup> S. Yang,<sup>17</sup> S. Jayatilake,<sup>18</sup> G. Mancinelli,<sup>18</sup> B. T. Meadows,<sup>18</sup> M. D. Sokoloff,<sup>18</sup> T. Barillari,<sup>19</sup> F. Blanc,<sup>19</sup> P. Bloom,<sup>19</sup> W. T. Ford,<sup>19</sup> U. Nauenberg,<sup>19</sup> A. Olivas,<sup>19</sup> P. Rankin,<sup>19</sup> J. Roy,<sup>19</sup> J. G. Smith,<sup>19</sup> W. C. van Hoek,<sup>19</sup> L. Zhang,<sup>19</sup> J. L. Harton,<sup>20</sup> T. Hu,<sup>20</sup> A. Soffer,<sup>20</sup> W. H. Toki,<sup>20</sup> R. J. Wilson,<sup>20</sup> J. Zhang,<sup>20</sup> D. Altenburg,<sup>21</sup> T. Brandt,<sup>21</sup> J. Brose,<sup>21</sup> T. Colberg,<sup>21</sup> M. Dickopp,<sup>21</sup> R. S. Dubitzky,<sup>21</sup> A. Hauke,<sup>21</sup> E. Maly,<sup>21</sup> R. Müller-Pfefferkorn,<sup>21</sup> R. Nogowski,<sup>21</sup> S. Otto,<sup>21</sup> K. R. Schubert,<sup>21</sup> R. Schwierz,<sup>21</sup> B. Spaan,<sup>21</sup> L. Wilden,<sup>21</sup> D. Bernard,<sup>22</sup> G. R. Bonneaud,<sup>22</sup> F. Brochard,<sup>22</sup> J. Cohen-Tanugi,<sup>22</sup> S. T'Jampens,<sup>22</sup> Ch. Thiebaux,<sup>22</sup> G. Vasileiadis,<sup>22</sup> M. Verderi,<sup>22</sup> A. Anjomshoa,<sup>23</sup> R. Bernet,<sup>23</sup> A. Khan,<sup>23</sup> D. Lavin,<sup>23</sup> F. Muheim,<sup>23</sup> S. Playfer,<sup>23</sup> J. E. Swain,<sup>23</sup> J. Tinslay,<sup>23</sup> M. Falbo,<sup>24</sup> C. Borean,<sup>25</sup> C. Bozzi,<sup>25</sup> L. Piemontese,<sup>25</sup> A. Sarti,<sup>25</sup> E. Treadwell,<sup>26</sup> F. Anulli,<sup>27</sup> \* R. Baldini-Feroli,<sup>27</sup> A. Calcaterra,<sup>27</sup> R. de Sangro,<sup>27</sup> D. Falciari,<sup>27</sup> G. Finocchiaro,<sup>27</sup> P. Patteri,<sup>27</sup> I. M. Peruzzi,<sup>27</sup> \* M. Piccolo,<sup>27</sup> A. Zallo,<sup>27</sup> S. Bagnasco,<sup>28</sup> A. Buzzo,<sup>28</sup> R. Contri,<sup>28</sup> G. Crosetti,<sup>28</sup> M. Lo Vetere,<sup>28</sup> M. Macri,<sup>28</sup> M. R. Monge,<sup>28</sup> S. Passaggio,<sup>28</sup> F. C. Pastore,<sup>28</sup> C. Patrignani,<sup>28</sup> E. Robutti,<sup>28</sup> A. Santroni,<sup>28</sup> S. Tosi,<sup>28</sup> S. Bailey,<sup>29</sup> M. Morii,<sup>29</sup> G. J. Grenier,<sup>30</sup> U. Mallik,<sup>30</sup> J. Cochran,<sup>31</sup> H. B. Crawley,<sup>31</sup> J. Lamsa,<sup>31</sup> W. T. Meyer,<sup>31</sup> S. Prell,<sup>31</sup> E. I. Rosenberg,<sup>31</sup> J. Yi,<sup>31</sup> M. Davier,<sup>32</sup> G. Grosdidier,<sup>32</sup> A. Höcker,<sup>32</sup> H. M. Lacker,<sup>32</sup> S. Laplace,<sup>32</sup> F. Le Diberder,<sup>32</sup> V. Lepeltier,<sup>32</sup> A. M. Lutz,<sup>32</sup> T. C. Petersen,<sup>32</sup> S. Plaszczynski,<sup>32</sup> M. H. Schune,<sup>32</sup> L. Tantot,<sup>32</sup> G. Wormser,<sup>32</sup> R. M. Bionta,<sup>33</sup> V. Brigljević,<sup>33</sup> D. J. Lange,<sup>33</sup> K. van Bibber,<sup>33</sup> D. M. Wright,<sup>33</sup> A. J. Bevan,<sup>34</sup> J. R. Fry,<sup>34</sup> E. Gabathuler,<sup>34</sup> R. Gamet,<sup>34</sup> M. George,<sup>34</sup> M. Kay,<sup>34</sup> D. J. Payne,<sup>34</sup> R. J. Sloane,<sup>34</sup> C. Touramanis,<sup>34</sup> M. L. Aspinwall,<sup>35</sup> D. A. Bowerman,<sup>35</sup> P. D. Dauncey,<sup>35</sup> U. Egede,<sup>35</sup> I. Eschrich,<sup>35</sup> G. W. Morton,<sup>35</sup> J. A. Nash,<sup>35</sup> P. Sanders,<sup>35</sup> G. P. Taylor,<sup>35</sup> J. J. Back,<sup>36</sup> G. Bellodi,<sup>36</sup> P. Dixon,<sup>36</sup> P. F. Harrison,<sup>36</sup> H. W. Shorthouse,<sup>36</sup> P. Strother,<sup>36</sup> P. B. Vidal,<sup>36</sup> G. Cowan,<sup>37</sup> H. U. Flaecher,<sup>37</sup> S. George,<sup>37</sup> M. G. Green,<sup>37</sup> A. Kurup,<sup>37</sup> C. E. Marker,<sup>37</sup> T. R. McMahon,<sup>37</sup> S. Ricciardi,<sup>37</sup> F. Salvatore,<sup>37</sup> G. Vaitas,<sup>37</sup> M. A. Winter,<sup>37</sup> D. Brown,<sup>38</sup> C. L. Davis,<sup>38</sup> J. Allison,<sup>39</sup> R. J. Barlow,<sup>39</sup> A. C. Forti,<sup>39</sup> P. A. Hart,<sup>39</sup> F. Jackson,<sup>39</sup> G. D. Lafferty,<sup>39</sup> A. J. Lyon,<sup>39</sup> N. Savvas,<sup>39</sup> J. H. Weatherall,<sup>39</sup> J. C. Williams,<sup>39</sup> A. Farbin,<sup>40</sup> A. Jawahery,<sup>40</sup> V. Lillard,<sup>40</sup> D. A. Roberts,<sup>40</sup> G. Blaylock,<sup>41</sup> C. Dallapiccola,<sup>41</sup> K. T. Flood,<sup>41</sup> S. S. Hertzbach,<sup>41</sup> R. Kofler,<sup>41</sup> V. B. Koptchev,<sup>41</sup> T. B. Moore,<sup>41</sup> H. Staengle,<sup>41</sup> S. Willocq,<sup>41</sup> R. Cowan,<sup>42</sup> G. Sciolla,<sup>42</sup> F. Taylor,<sup>42</sup> R. K. Yamamoto,<sup>42</sup> M. Milek,<sup>43</sup> P. M. Patel,<sup>43</sup> F. Palombo,<sup>44</sup> J. M. Bauer,<sup>45</sup> L. Cremaldi,<sup>45</sup> V. Eschenburg,<sup>45</sup> R. Kroeger,<sup>45</sup> J. Reidy,<sup>45</sup> D. A. Sanders,<sup>45</sup> D. J. Summers,<sup>45</sup> H. Zhao,<sup>45</sup> C. Hast,<sup>46</sup> P. Taras,<sup>46</sup> H. Nicholson,<sup>47</sup> C. Cartaro,<sup>48</sup> N. Cavallo,<sup>48</sup>

G. De Nardo,<sup>48</sup> F. Fabozzi,<sup>48,†</sup> C. Gatto,<sup>48</sup> L. Lista,<sup>48</sup> P. Paolucci,<sup>48</sup> D. Piccolo,<sup>48</sup> C. Sciacca,<sup>48</sup> J. M. LoSecco,<sup>49</sup> J. R. G. Alsmiller,<sup>50</sup> T. A. Gabriel,<sup>50</sup> B. Brau,<sup>51</sup> J. Brau,<sup>52</sup> R. Frey,<sup>52</sup> M. Iwasaki,<sup>52</sup> C. T. Potter,<sup>52</sup> N. B. Sinev,<sup>52</sup> D. Strom,<sup>52</sup> E. Torrence,<sup>52</sup> F. Colecchia,<sup>53</sup> A. Dorigo,<sup>53</sup> F. Galeazzi,<sup>53</sup> M. Margoni,<sup>53</sup> M. Morandini,<sup>53</sup> M. Posocco,<sup>53</sup> M. Rotondo,<sup>53</sup> F. Simonetto,<sup>53</sup> R. Stroili,<sup>53</sup> G. Tiozzo,<sup>53</sup> C. Voci,<sup>53</sup> M. Benayoun,<sup>54</sup> H. Briand,<sup>54</sup> J. Chauveau,<sup>54</sup> P. David,<sup>54</sup> Ch. de la Vaissière,<sup>54</sup> L. Del Buono,<sup>54</sup> O. Hamon,<sup>54</sup> Ph. Leruste,<sup>54</sup> J. Ocariz,<sup>54</sup> M. Pivk,<sup>54</sup> L. Roos,<sup>54</sup> J. Stark,<sup>54</sup> P. F. Manfredi,<sup>55</sup> V. Re,<sup>55</sup> V. Speziali,<sup>55</sup> L. Gladney,<sup>56</sup> Q. H. Guo,<sup>56</sup> J. Panetta,<sup>56</sup> C. Angelini,<sup>57</sup> G. Batignani,<sup>57</sup> S. Bettarini,<sup>57</sup> M. Bondioli,<sup>57</sup> F. Bucci,<sup>57</sup> G. Calderini,<sup>57</sup> E. Campagna,<sup>57</sup> M. Carpinelli,<sup>57</sup> F. Forti,<sup>57</sup> M. A. Giorgi,<sup>57</sup> A. Lusiani,<sup>57</sup> G. Marchiori,<sup>57</sup> F. Martinez-Vidal,<sup>57</sup> M. Morganti,<sup>57</sup> N. Neri,<sup>57</sup> E. Paoloni,<sup>57</sup> M. Rama,<sup>57</sup> G. Rizzo,<sup>57</sup> F. Sandrelli,<sup>57</sup> G. Triggiani,<sup>57</sup> J. Walsh,<sup>57</sup> M. Haire,<sup>58</sup> D. Judd,<sup>58</sup> K. Paick,<sup>58</sup> L. Turnbull,<sup>58</sup> D. E. Wagoner,<sup>58</sup> N. Danielson,<sup>59</sup> P. Elmer,<sup>59</sup> C. Lu,<sup>59</sup> V. Miftakov,<sup>59</sup> J. Olsen,<sup>59</sup> A. J. S. Smith,<sup>59</sup> A. Tumanov,<sup>59</sup> E. W. Varnes,<sup>59</sup> F. Bellini,<sup>60</sup> G. Cavoto,<sup>59,60</sup> D. del Re,<sup>60</sup> R. Faccini,<sup>14,60</sup> F. Ferrarotto,<sup>60</sup> F. Ferroni,<sup>60</sup> M. Gaspero,<sup>60</sup> E. Leonardi,<sup>60</sup> M. A. Mazzoni,<sup>60</sup> S. Morganti,<sup>60</sup> G. Piredda,<sup>60</sup> F. Safai Tehrani,<sup>60</sup> M. Serra,<sup>60</sup> C. Voena,<sup>60</sup> S. Christ,<sup>61</sup> G. Wagner,<sup>61</sup> R. Waldi,<sup>61</sup> T. Adye,<sup>62</sup> N. De Groot,<sup>62</sup> B. Franek,<sup>62</sup> N. I. Geddes,<sup>62</sup> G. P. Gopal,<sup>62</sup> E. O. Olaiya,<sup>62</sup> S. M. Xella,<sup>62</sup> R. Aleksan,<sup>63</sup> S. Emery,<sup>63</sup> A. Gaidot,<sup>63</sup> P.-F. Giraud,<sup>63</sup> G. Hamel de Monchenault,<sup>63</sup> W. Kozanecki,<sup>63</sup> M. Langer,<sup>63</sup> G. W. London,<sup>63</sup> B. Mayer,<sup>63</sup> G. Schott,<sup>63</sup> B. Serfass,<sup>63</sup> G. Vasseur,<sup>63</sup> Ch. Yeche,<sup>63</sup> M. Zito,<sup>63</sup> M. V. Purohit,<sup>64</sup> F. X. Yumiceva,<sup>64</sup> A. W. Weidemann,<sup>64</sup> K. Abe,<sup>65</sup> D. Aston,<sup>65</sup> R. Bartoldus,<sup>65</sup> N. Berger,<sup>65</sup> A. M. Boyarski,<sup>65</sup> O. L. Buchmueller,<sup>65</sup> M. R. Convery,<sup>65</sup> D. P. Coupal,<sup>65</sup> D. Dong,<sup>65</sup> J. Dorfan,<sup>65</sup> W. Dunwoodie,<sup>65</sup> R. C. Field,<sup>65</sup> T. Glanzman,<sup>65</sup> S. J. Gowdy,<sup>65</sup> E. Grauges-Pous,<sup>65</sup> T. Hadig,<sup>65</sup> V. Halyo,<sup>65</sup> T. Himel,<sup>65</sup> T. Hryn'ova,<sup>65</sup> M. E. Huffer,<sup>65</sup> W. R. Innes,<sup>65</sup> C. P. Jessop,<sup>65</sup> M. H. Kelsey,<sup>65</sup> P. Kim,<sup>65</sup> M. L. Kocian,<sup>65</sup> U. Langenegger,<sup>65</sup> D. W. G. S. Leith,<sup>65</sup> S. Luitz,<sup>65</sup> V. Luth,<sup>65</sup> H. L. Lynch,<sup>65</sup> H. Marsiske,<sup>65</sup> S. Menke,<sup>65</sup> R. Messner,<sup>65</sup> D. R. Muller,<sup>65</sup> C. P. O'Grady,<sup>65</sup> V. E. Ozcan,<sup>65</sup> A. Perazzo,<sup>65</sup> M. Perl,<sup>65</sup> S. Petrak,<sup>65</sup> B. N. Ratcliff,<sup>65</sup> S. H. Robertson,<sup>65</sup> A. Roodman,<sup>65</sup> A. A. Salnikov,<sup>65</sup> T. Schietinger,<sup>65</sup> R. H. Schindler,<sup>65</sup> J. Schwiening,<sup>65</sup> G. Simi,<sup>65</sup> A. Snyder,<sup>65</sup> A. Soha,<sup>65</sup> J. Stelzer,<sup>65</sup> D. Su,<sup>65</sup> M. K. Sullivan,<sup>65</sup> H. A. Tanaka,<sup>65</sup> J. Va'vra,<sup>65</sup> S. R. Wagner,<sup>65</sup> M. Weaver,<sup>65</sup> A. J. R. Weinstein,<sup>65</sup> W. J. Wisniewski,<sup>65</sup> D. H. Wright,<sup>65</sup> C. C. Young,<sup>65</sup> P. R. Burchat,<sup>66</sup> C. H. Cheng,<sup>66</sup> T. I. Meyer,<sup>66</sup> C. Roat,<sup>66</sup> W. Bugg,<sup>67</sup> M. Krishnamurthy,<sup>67</sup> S. M. Spanier,<sup>67</sup> J. M. Izen,<sup>68</sup> I. Kitayama,<sup>68</sup> X. C. Lou,<sup>68</sup> F. Bianchi,<sup>69</sup> M. Bona,<sup>69</sup> D. Gamba,<sup>69</sup> L. Bosisio,<sup>70</sup> G. Della Ricca,<sup>70</sup> S. Dittongo,<sup>70</sup> L. Lanceri,<sup>70</sup> P. Poropat,<sup>70</sup> L. Vitale,<sup>70</sup> G. Vuagnin,<sup>70</sup> R. Henderson,<sup>71</sup> R. S. Panvini,<sup>72</sup> Sw. Banerjee,<sup>73</sup> C. M. Brown,<sup>73</sup> D. Fortin,<sup>73</sup> P. D. Jackson,<sup>73</sup> R. Kowalewski,<sup>73</sup> J. M. Roney,<sup>73</sup> H. R. Band,<sup>74</sup> S. Dasu,<sup>74</sup> M. Datta,<sup>74</sup> A. M. Eichenbaum,<sup>74</sup> H. Hu,<sup>74</sup> J. R. Johnson,<sup>74</sup> R. Liu,<sup>74</sup> F. Di Lodovico,<sup>74</sup> A. K. Mohapatra,<sup>74</sup> Y. Pan,<sup>74</sup> R. Prepost,<sup>74</sup> S. J. Sekula,<sup>74</sup> J. H. von Wimmersperg-Toeller,<sup>74</sup> J. Wu,<sup>74</sup> S. L. Wu,<sup>74</sup> Z. Yu,<sup>74</sup> and H. Neal<sup>75</sup>

(The BABAR Collaboration)

<sup>1</sup>Laboratoire de Physique des Particules, F-74941 Annecy-le-Vieux, France

<sup>2</sup>Università di Bari, Dipartimento di Fisica and INFN, I-70126 Bari, Italy

<sup>3</sup>Institute of High Energy Physics, Beijing 100039, China

<sup>4</sup>University of Bergen, Inst. of Physics, N-5007 Bergen, Norway

<sup>5</sup>Lawrence Berkeley National Laboratory and University of California, Berkeley, CA 94720, USA

<sup>6</sup>University of Birmingham, Birmingham, B15 2TT, United Kingdom

<sup>7</sup>Ruhr Universität Bochum, Institut für Experimentalphysik 1, D-44780 Bochum, Germany

<sup>8</sup>University of Bristol, Bristol BS8 1TL, United Kingdom

<sup>9</sup>University of British Columbia, Vancouver, BC, Canada V6T 1Z1

<sup>10</sup>Brunel University, Uxbridge, Middlesex UB8 3PH, United Kingdom

<sup>11</sup>Budker Institute of Nuclear Physics, Novosibirsk 630090, Russia

<sup>12</sup>University of California at Irvine, Irvine, CA 92697, USA

<sup>13</sup>University of California at Los Angeles, Los Angeles, CA 90024, USA

<sup>14</sup>University of California at San Diego, La Jolla, CA 92093, USA

<sup>15</sup>University of California at Santa Barbara, Santa Barbara, CA 93106, USA

<sup>16</sup>University of California at Santa Cruz, Institute for Particle Physics, Santa Cruz, CA 95064, USA

<sup>17</sup>California Institute of Technology, Pasadena, CA 91125, USA

<sup>18</sup>University of Cincinnati, Cincinnati, OH 45221, USA

<sup>19</sup>University of Colorado, Boulder, CO 80309, USA

<sup>20</sup>Colorado State University, Fort Collins, CO 80523, USA

<sup>21</sup>Technische Universität Dresden, Institut für Kern- und Teilchenphysik, D-01062 Dresden, Germany

<sup>22</sup>Ecole Polytechnique, LLR, F-91128 Palaiseau, France

<sup>23</sup>University of Edinburgh, Edinburgh EH9 3JZ, United Kingdom

<sup>24</sup>Elon University, Elon University, NC 27244-2010, USA

- <sup>25</sup> *Università di Ferrara, Dipartimento di Fisica and INFN, I-44100 Ferrara, Italy*  
<sup>26</sup> *Florida A&M University, Tallahassee, FL 32307, USA*  
<sup>27</sup> *Laboratori Nazionali di Frascati dell'INFN, I-00044 Frascati, Italy*  
<sup>28</sup> *Università di Genova, Dipartimento di Fisica and INFN, I-16146 Genova, Italy*  
<sup>29</sup> *Harvard University, Cambridge, MA 02138, USA*  
<sup>30</sup> *University of Iowa, Iowa City, IA 52242, USA*  
<sup>31</sup> *Iowa State University, Ames, IA 50011-3160, USA*  
<sup>32</sup> *Laboratoire de l'Accélérateur Linéaire, F-91898 Orsay, France*  
<sup>33</sup> *Lawrence Livermore National Laboratory, Livermore, CA 94550, USA*  
<sup>34</sup> *University of Liverpool, Liverpool L69 3BX, United Kingdom*  
<sup>35</sup> *University of London, Imperial College, London, SW7 2BW, United Kingdom*  
<sup>36</sup> *Queen Mary, University of London, E1 4NS, United Kingdom*  
<sup>37</sup> *University of London, Royal Holloway and Bedford New College, Egham, Surrey TW20 0EX, United Kingdom*  
<sup>38</sup> *University of Louisville, Louisville, KY 40292, USA*  
<sup>39</sup> *University of Manchester, Manchester M13 9PL, United Kingdom*  
<sup>40</sup> *University of Maryland, College Park, MD 20742, USA*  
<sup>41</sup> *University of Massachusetts, Amherst, MA 01003, USA*  
<sup>42</sup> *Massachusetts Institute of Technology, Laboratory for Nuclear Science, Cambridge, MA 02139, USA*  
<sup>43</sup> *McGill University, Montréal, QC, Canada H3A 2T8*  
<sup>44</sup> *Università di Milano, Dipartimento di Fisica and INFN, I-20133 Milano, Italy*  
<sup>45</sup> *University of Mississippi, University, MS 38677, USA*  
<sup>46</sup> *Université de Montréal, Laboratoire René J. A. Lévesque, Montréal, QC, Canada H3C 3J7*  
<sup>47</sup> *Mount Holyoke College, South Hadley, MA 01075, USA*  
<sup>48</sup> *Università di Napoli Federico II, Dipartimento di Scienze Fisiche and INFN, I-80126, Napoli, Italy*  
<sup>49</sup> *University of Notre Dame, Notre Dame, IN 46556, USA*  
<sup>50</sup> *Oak Ridge National Laboratory, Oak Ridge, TN 37831, USA*  
<sup>51</sup> *Ohio State Univ., 174 W.18th Ave., Columbus, OH 43210*  
<sup>52</sup> *University of Oregon, Eugene, OR 97403, USA*  
<sup>53</sup> *Università di Padova, Dipartimento di Fisica and INFN, I-35131 Padova, Italy*  
<sup>54</sup> *Universités Paris VI et VII, Lab de Physique Nucléaire H. E., F-75252 Paris, France*  
<sup>55</sup> *Università di Pavia, Dipartimento di Elettronica and INFN, I-27100 Pavia, Italy*  
<sup>56</sup> *University of Pennsylvania, Philadelphia, PA 19104, USA*  
<sup>57</sup> *Università di Pisa, Scuola Normale Superiore and INFN, I-56010 Pisa, Italy*  
<sup>58</sup> *Prairie View A&M University, Prairie View, TX 77446, USA*  
<sup>59</sup> *Princeton University, Princeton, NJ 08544, USA*  
<sup>60</sup> *Università di Roma La Sapienza, Dipartimento di Fisica and INFN, I-00185 Roma, Italy*  
<sup>61</sup> *Universität Rostock, D-18051 Rostock, Germany*  
<sup>62</sup> *Rutherford Appleton Laboratory, Chilton, Didcot, Oxon, OX11 0QX, United Kingdom*  
<sup>63</sup> *DAPNIA, Commissariat à l'Energie Atomique/Saclay, F-91191 Gif-sur-Yvette, France*  
<sup>64</sup> *University of South Carolina, Columbia, SC 29208, USA*  
<sup>65</sup> *Stanford Linear Accelerator Center, Stanford, CA 94309, USA*  
<sup>66</sup> *Stanford University, Stanford, CA 94305-4060, USA*  
<sup>67</sup> *University of Tennessee, Knoxville, TN 37996, USA*  
<sup>68</sup> *University of Texas at Dallas, Richardson, TX 75083, USA*  
<sup>69</sup> *Università di Torino, Dipartimento di Fisica Sperimentale and INFN, I-10125 Torino, Italy*  
<sup>70</sup> *Università di Trieste, Dipartimento di Fisica and INFN, I-34127 Trieste, Italy*  
<sup>71</sup> *TRIUMF, Vancouver, BC, Canada V6T 2A3*  
<sup>72</sup> *Vanderbilt University, Nashville, TN 37235, USA*  
<sup>73</sup> *University of Victoria, Victoria, BC, Canada V8W 3P6*  
<sup>74</sup> *University of Wisconsin, Madison, WI 53706, USA*  
<sup>75</sup> *Yale University, New Haven, CT 06511, USA*

(Dated: October 24, 2018)

The neutral  $B$  meson lifetime is measured with the data collected by the BABAR detector at the PEP-II storage ring during the years 1999 and 2000, with a total integrated luminosity of  $20.7 \text{ fb}^{-1}$ . The decays  $B^0 \rightarrow D^{*-}\pi^+$  and  $B^0 \rightarrow D^{*-}\rho^+$  are selected with a partial-reconstruction technique, yielding samples of  $6970 \pm 240$  and  $5520 \pm 250$  signal events, respectively. With these events, the  $B^0$  lifetime is measured to be  $1.533 \pm 0.034$  (stat.)  $\pm 0.038$  (syst.) ps. This measurement serves as a test and validation of procedures required to measure the  $CP$  violation parameter  $\sin(2\beta + \gamma)$  with partial reconstruction of these modes.

PACS numbers: 13.25.Hw, 12.15.Hh, 11.30.Er

The neutral  $B$  meson decay modes [1]  $B^0 \rightarrow D^{*-}h^+$ , where  $h^+$  is a light hadron ( $\pi^+, \rho^+, a_1^+$ ), have been pro-

posed for use in theoretically clean measurements of  $\sin(2\beta + \gamma)$  [2], where  $(2\beta + \gamma)$  is a combination of angles of the Cabibbo-Kobayashi-Maskawa [3] unitarity triangle. Since the time-dependent  $CP$  asymmetries in these modes are expected to be of order 2%, large data samples and multiple decay channels are required for a statistically significant measurement. The technique of partial reconstruction of  $D^{*-}$  mesons, in which only the soft pion  $\pi_s$  from the decay  $D^{*-} \rightarrow \bar{D}^0 \pi_s^-$  is reconstructed, has already been used to select large samples of  $B$  meson candidates [4]. This technique is applied here to the decays  $B^0 \rightarrow D^{*-} \pi^+$  and  $B^0 \rightarrow D^{*-} \rho^+$  in order to measure the  $B^0$  lifetime. This analysis constitutes a first step toward measuring  $\sin(2\beta + \gamma)$ , validating the procedures developed for candidate reconstruction, background characterization, vertex reconstruction, and fitting of decay time distributions. These procedures address the main complications introduced by partial reconstruction, namely the large background and the tracks originating from the unreconstructed  $\bar{D}^0$ , which may affect the vertex reconstruction.

The analyses applied to the  $B^0 \rightarrow D^{*-} \pi^+$  and  $B^0 \rightarrow D^{*-} \rho^+$  modes are similar. Detailed differences between them are the result of optimization in the presence of the different background characteristics in the two modes. Additional details regarding the analysis procedures can be found in Refs. [5] and [6].

The data used in this analysis were collected with the *BABAR* detector at the PEP-II asymmetric-energy storage ring during the years 1999 and 2000. The data consist of 22.7 million  $B\bar{B}$  pairs, corresponding to an integrated luminosity of  $20.7 \text{ fb}^{-1}$  recorded at the  $\Upsilon(4S)$  resonance. In addition,  $2.6 \text{ fb}^{-1}$  of “off-resonance” data were collected about 40 MeV below the resonance. Samples of simulated  $B\bar{B}$  and continuum  $e^+e^- \rightarrow q\bar{q}$  events, where  $q$  stands for a  $u$ ,  $d$ ,  $s$ , or  $c$  quark, were generated using a GEANT3-based detector simulation [7] and processed through the same reconstruction and analysis chain as the data. The equivalent luminosity of the simulated events is approximately one third the data luminosity. We also used signal Monte Carlo samples with an equivalent luminosity several times larger than that of the data.

The *BABAR* detector, described in detail elsewhere [8], consists of five subdetectors. Charged particle trajectories are measured by a combination of a five-layer silicon vertex tracker (SVT) and a 40-layer drift chamber (DCH) in a 1.5 T solenoidal magnetic field. Tracks with low transverse momentum are reconstructed by the SVT alone, thus extending the charged particle detection down to transverse momenta of  $\sim 50 \text{ MeV}/c$ . Photons and electrons are detected in a CsI(Tl) electromagnetic calorimeter (EMC), with photon energy resolution  $\sigma_E/E = 0.023(E/\text{GeV})^{-1/4} \oplus 0.019$ . A ring-imaging Cherenkov detector (DIRC) is used for charged particle identification. The instrumented flux return (IFR) is

equipped with resistive plate chambers to identify muons.

In the partial reconstruction of a  $B^0 \rightarrow D^{*-} h^+$  candidate, only the hadron  $h$  and the  $\pi_s$  tracks are reconstructed. The angle between the momenta of the  $B$  and the  $h$  in the center-of-mass (CM) frame is then computed:

$$\cos \theta_{Bh} = \frac{M_{D^{*-}}^2 - M_{B^0}^2 - M_h^2 + E_{\text{CM}} E_h}{2p_B |\vec{p}_h|}, \quad (1)$$

where  $M_x$  is the mass of particle  $x$ ,  $E_h$  and  $\vec{p}_h$  are the measured CM energy and momentum of the hadron  $h$ ,  $E_{\text{CM}}$  is the total CM energy of the beams, and  $p_B = \sqrt{E_{\text{CM}}^2/4 - M_{B^0}^2}$ . All masses refer to the nominal values [9], except in the case  $h = \rho$ , where the measured  $\pi^+ \pi^0$  invariant mass  $m(\pi^+ \pi^0)$  is used. Events are required to be in the physical region  $|\cos \theta_{Bh}| < 1$ . Given  $\cos \theta_{Bh}$  and the measured four-momentum of  $h$ , the  $B$  four-momentum can be calculated up to an unknown azimuthal angle  $\phi$  around  $\vec{p}_h$ . For every value of  $\phi$ , the expected  $\bar{D}^0$  four-momentum  $\mathcal{P}_D(\phi)$  is determined from four-momentum conservation, and the  $\phi$ -dependent “missing mass” is calculated,  $m(\phi) \equiv \sqrt{|\mathcal{P}_D(\phi)|^2}$ . We define the missing mass  $m_{\text{miss}} \equiv \frac{1}{2} [m_{\text{max}} + m_{\text{min}}]$ , where  $m_{\text{max}}$  and  $m_{\text{min}}$  are the maximum and minimum values of  $m(\phi)$ . In signal events, this variable peaks at the nominal  $\bar{D}^0$  mass  $M_{D^0}$ , with a spread of about  $3 \text{ MeV}/c^2$  for  $B^0 \rightarrow D^{*-} \pi^+$  ( $3.5 \text{ MeV}/c^2$  for  $B^0 \rightarrow D^{*-} \rho^+$ ) [10], while the distribution of background events is broader. The missing mass is the main variable used to distinguish signal from background.

We define the  $D^*$  helicity angle  $\theta_{D^*}$  to be the angle between the directions of the  $\bar{D}^0$  and the  $B^0$  in the  $D^*$  rest frame. This variable is used in the event selection described below. In the  $B^0 \rightarrow D^{*-} \pi^+$  analysis,  $\theta_{D^*}$  is computed assuming that the  $B$  momentum lies in the plane defined by the  $h$  and  $\pi_s$  momenta in the CM frame. This assumption also yields the  $\bar{D}^0$  direction. In the  $B^0 \rightarrow D^{*-} \rho^+$  analysis, the value of  $\cos \theta_{D^*}$  is computed by applying the constraint  $m_{\text{miss}} = M_{D^0}$  giving two possible solutions for the  $\bar{D}^0$  direction [4]. In  $B^0 \rightarrow D^{*-} \rho^+$ , the  $\rho$  helicity angle  $\theta_\rho$  is defined as the angle between the directions of the  $\pi^0$  (from the decay of the  $\rho$ ) and the CM system in the  $\rho$  rest frame.

We select events in which the ratio of the 2nd to the 0th Fox-Wolfram moment [11], computed using charged particles, is smaller than 0.35. The candidate  $B^0$  daughter tracks are required to originate within 1 cm (1.5 cm) of the interaction point in the  $x$ - $y$  plane (the plane perpendicular to the beams), and within  $\pm 4$  cm ( $\pm 10$  cm) of the interaction point along the direction of the beams. Tracks are rejected if they are highly likely to be a kaon or a lepton on the basis of their ionization, Cherenkov angle, energy deposited in the EMC, and pattern of hits in the IFR.

$B^0 \rightarrow D^{*-} \pi^+$  candidates are rejected if another track

is found within 0.4 rad of the momentum of the hard pion  $\pi_h$  [12] in the CM frame. This requirement helps to reject continuum events, where tracks tend to be clustered in jets. A Fisher discriminant [13]  $F_\pi$  is computed from 15 event shape variables. Among these variables is the scalar sum of the CM momenta of all tracks and neutral candidates in nine  $20^\circ$  single-sided cones around the  $\pi_h$  direction. We require  $|\cos\theta_{D^*}|$  to be larger than 0.4. A cut on  $F_\pi$  is used to reduce the continuum background.

In the reconstruction of  $B^0 \rightarrow D^{*-}\rho^+$  candidates, the charged  $\rho$  candidates are identified by their decay to a hard charged pion  $\pi_h$  and a  $\pi^0$ . To suppress fake  $\pi^0$  candidates, the  $\pi^0$  momentum in the CM frame is required to be greater than  $400 \text{ MeV}/c$ . The invariant mass of the  $\pi^0 \rightarrow \gamma\gamma$  candidate must be within  $20 \text{ MeV}/c^2$  of the nominal  $\pi^0$  mass [9]. The invariant mass  $m(\pi^+\pi^0)$  of the  $\rho$  candidate must be between 0.45 and  $1.10 \text{ GeV}/c^2$ . To suppress combinatoric background, we require  $|\cos\theta_\rho| > 0.3$  and  $|\cos\theta_{D^*}| > 0.3$ , and also reject events that satisfy both  $\cos\theta_\rho > 0.3$  and  $\cos\theta_{D^*} < -0.3$ . A Fisher discriminant  $F_\rho$  is computed using the scalar sum of the CM momenta of all tracks and neutrals in nine  $10^\circ$  double-sided cones around the  $\rho$  direction. In about 10% of the events, more than one partially reconstructed candidate per event satisfies all the requirements. In such events only the candidate with the smallest value of  $|m_{\text{miss}} - M_{D^0}|$  in the event is used.

The decay position  $z_{\text{rec}}$  of the partially reconstructed  $B$  candidate along the beam direction is determined by constraining the  $\pi_h$  and the  $\pi_s$  tracks (only the  $\pi_h$  track for  $B^0 \rightarrow D^{*-}\rho^+$ ) to originate from the beam-spot in the  $x$ - $y$  plane. The beam spot is determined on a run-by-run basis using two-prong events [8]. Its size in the horizontal direction is  $120 \mu\text{m}$ . Although the beam spot size in the vertical direction is only a few microns, a beam spot constraint of  $30 \mu\text{m}$  is applied, so as to account for the flight of the  $B^0$  in the vertical direction.

The decay position  $z_{\text{other}}$  of the other  $B$  meson along the beam direction is measured with all tracks, excluding  $\pi_h$ ,  $\pi_s$ , and any track whose CM angle with respect to the  $\bar{D}^0$  direction (either of the two calculated directions in the  $B^0 \rightarrow D^{*-}\rho^+$  case) is smaller than 1 radian. This ‘‘cone cut’’ reduces significantly the number of  $\bar{D}^0$  daughter tracks used in the other  $B$  vertex. The tracks satisfying this requirement are fit with a constraint to the beam-spot in the  $x$ – $y$  plane. The track with the largest contribution to the  $\chi^2$  of the vertex, if greater than 6, is removed from the vertex, and the fit is carried out again, until no track fails this requirement.  $B^0 \rightarrow D^{*-}\pi^+$  candidates are required to have at least two tracks remaining in the other  $B$  vertex.

The  $z$  distance between the two  $B$  decay vertices,  $\Delta z = z_{\text{rec}} - z_{\text{other}}$ , is computed. Fitting the residual  $\Delta z - \Delta z_{\text{true}}$  in simulated events, where  $\Delta z_{\text{true}}$  is the true  $\Delta z$ , with the sum of two Gaussians, we find that 67% (57%) of the  $B^0 \rightarrow D^{*-}\pi^+$  ( $B^0 \rightarrow D^{*-}\rho^+$ ) events

lie in the core Gaussian of width  $116 \mu\text{m}$  ( $178 \mu\text{m}$ ). The  $\Delta z$  resolution is dominated by the measurement of  $z_{\text{other}}$ , and by the  $z_{\text{rec}}$  measurement when the  $\pi_h$  transverse momentum is below about  $400 \text{ MeV}/c$ .

The decay time difference  $\Delta t$  is then calculated using the approximation  $\Delta t \approx \Delta z/(\gamma\beta c)$ , where the CM frame boost  $\gamma\beta$  is determined from the beam energies, and has an average value of 0.55. This approximation results in a  $0.2 \text{ ps}$  r.m.s. spread in the calculation of  $\Delta t$ .

For  $B^0 \rightarrow D^{*-}\pi^+$  candidates,  $\Delta t$  is computed applying an event-by-event correction to the measured value of  $\Delta z$ . This correction, determined from the simulated signal sample as a function of  $\Delta z$ , removes the bias in  $z_{\text{other}}$  due to the tracks coming from the  $\bar{D}^0$  decay. Without correction, the effect of this bias would be to reduce the measured lifetime by approximately 4%. In the  $B^0 \rightarrow D^{*-}\rho^+$  analysis a different correction is applied to the measured lifetime value, as explained later.

The estimated error  $\sigma_{\Delta t}$  in the measurement of  $\Delta t$  is calculated from the uncertainties in the parameters of the tracks used in the two vertex fits. A requirement on the vertex fit probabilities removes badly reconstructed vertices. For both modes we also require  $|\Delta t| < 15 \text{ ps}$  and  $\sigma_{\Delta t} < 2.4 \text{ ps}$  ( $\sigma_{\Delta t} < 4 \text{ ps}$  for  $B^0 \rightarrow D^{*-}\rho^+$ ).

After applying all the above requirements, we find four broadly-defined types of events that contribute to the background: (1) continuum events; (2) combinatoric  $B\bar{B}$  background due to random  $h$  and  $\pi_s$  combinations; (3)  $B^0 \rightarrow D^{*-}\rho^+$  ( $B^0 \rightarrow D^{*-}a_1^+$ ) decays in the  $B^0 \rightarrow D^{*-}\pi^+$  ( $B^0 \rightarrow D^{*-}\rho^+$ ) sample; (4) peaking  $B\bar{B}$  events, which are distributed as a broad peak in the  $m_{\text{miss}}$  spectrum. The peaking background is mostly due to  $B \rightarrow D^{**}\pi$  decays in the  $B^0 \rightarrow D^{*-}\pi^+$  sample. In the  $B^0 \rightarrow D^{*-}\rho^+$  sample, it is due to signal events in which the  $\pi_h$  candidate originates from the other  $B$ .

The lifetime  $\tau_{B^0}$  is obtained from an unbinned maximum likelihood fit, as described below, with a probability density function (PDF)  $\mathcal{F}(\Delta t, \sigma_{\Delta t}, \xi)$ . Here  $\xi$  refers to the kinematic variables used to distinguish signal from background. For  $B^0 \rightarrow D^{*-}\pi^+$  we set  $\xi = m_{\text{miss}}$ ; for  $B^0 \rightarrow D^{*-}\rho^+$  we set  $\xi = (m_{\text{miss}}, m(\pi^+\pi^0), F_\rho)$ . The PDF has the form

$$\begin{aligned} \mathcal{F}(\xi, \Delta t, \sigma_{\Delta t}) = & f_{\text{cont}} \mathcal{K}_{\text{cont}}(\xi) \mathcal{F}_{\text{cont}}(\Delta t, \sigma_{\Delta t}) \\ & + f_{\text{comb}} \mathcal{K}_{\text{comb}}(\xi) \mathcal{F}_{\text{comb}}(\Delta t, \sigma_{\Delta t}) \\ & + f_{D^*X} \mathcal{K}_{D^*X}(\xi) \mathcal{F}_{D^*X}(\Delta t, \sigma_{\Delta t}) \\ & + f_{\text{peak}} \mathcal{K}_{\text{peak}}(\xi) \mathcal{F}_{\text{peak}}(\Delta t, \sigma_{\Delta t}) \\ & + f_{\text{sig}} \mathcal{K}_{\text{sig}}(\xi) \mathcal{F}_{\text{sig}}(\Delta t, \sigma_{\Delta t}), \end{aligned} \quad (2)$$

where subscripts refer to the four types of backgrounds enumerated above and to signal events. For each event type  $i$ ,  $f_i$  is the relative population of these events in the data sample,  $\mathcal{K}_i(\xi)$  is their kinematic-variables PDF, and  $\mathcal{F}_i(\Delta t, \sigma_{\Delta t})$  is their time-dependent PDF. The constraint  $\sum f_i = 1$  is enforced.

For  $B^0 \rightarrow D^{*-}\pi^+$ ,  $\mathcal{K}_i(m_{\text{miss}})$  consists of binned histograms obtained from the Monte Carlo simulation. For  $B^0 \rightarrow D^{*-}\rho^+$  candidates, we use the product  $\mathcal{K}_i(\xi) = \mathcal{M}_i(m_{\text{miss}})\mathcal{R}_i(m(\pi^+\pi^0))\mathcal{D}_i(F_\rho)$ , where  $\mathcal{M}_i(m_{\text{miss}})$  is the sum of a bifurcated Gaussian and an ARGUS function [14],  $\mathcal{R}_i(m(\pi^+\pi^0))$  is the sum of a parabolic background and a relativistic  $P$ -wave Breit-Wigner, and  $\mathcal{D}_i(F_\rho)$  is a bifurcated Gaussian function.

For each event type  $i$ ,  $\mathcal{F}_i(\Delta t, \sigma_{\Delta t})$  is the convolution  $N \int P(\Delta t_{\text{true}})R((\Delta t - \Delta t_{\text{true}})/\sigma_{\Delta t})d\Delta t_{\text{true}}$  of the “true” distribution  $P(\Delta t_{\text{true}})$  and the detector resolution function  $R((\Delta t - \Delta t_{\text{true}})/\sigma_{\Delta t})$ , which is parameterized as the sum of three Gaussian distributions.  $N$  is a normalization constant. The parameters of  $P(\Delta t_{\text{true}})$  and  $R((\Delta t - \Delta t_{\text{true}})/\sigma_{\Delta t})$  are obtained separately for each event type. For signal events of both modes we take  $P(\Delta t_{\text{true}}) = e^{-|\Delta t_{\text{true}}|/\tau_{B^0}}$ . This functional form is also used for the combinatoric and peaking backgrounds in  $B^0 \rightarrow D^{*-}\pi^+$ , but with independent parameters. In  $B^0 \rightarrow D^{*-}\rho^+$ , the source of the peaking background motivates its distribution to be  $P(\Delta t_{\text{true}}) = \delta(\Delta t_{\text{true}})$ , and the distribution used for the combinatoric background is  $P(\Delta t_{\text{true}}) = ae^{-|\Delta t_{\text{true}}|/\tau'} + (1-a)\delta(\Delta t_{\text{true}})$ , with an effective lifetime parameter  $\tau'$ .  $\mathcal{F}_{D^*X}(\Delta t, \sigma_{\Delta t})$  is assumed to be identical to  $\mathcal{F}_{\text{sig}}(\Delta t, \sigma_{\Delta t})$ . The continuum background is modelled as  $P(\Delta t_{\text{true}}) = be^{-|\Delta t_{\text{true}}|/\tau_{\text{cont}}} + (1-b)\delta(\Delta t_{\text{true}})$ .

Several subsamples are defined and used in the lifetime fit. Events with a candidate in which the  $h$  and  $\pi_s$  have opposite charges and with  $m_{\text{miss}} > 1.860 \text{ GeV}/c^2$  ( $m_{\text{miss}} > 1.845 \text{ GeV}/c^2$  in  $B^0 \rightarrow D^{*-}\rho^+$ ) constitute the “signal region” sample. Those satisfying  $1.820 < m_{\text{miss}} < 1.850 \text{ GeV}/c^2$  ( $1.810 < m_{\text{miss}} < 1.840 \text{ GeV}/c^2$ ) constitute the “sideband”. Events in which  $h$  and  $\pi_s$  have the same charge are labeled as “same-charge”. In the  $B^0 \rightarrow D^{*-}\pi^+$  analysis, we apply a requirement on the Fisher discriminant that suppresses  $B\bar{B}$  events, to select a “ $B\bar{B}$ -depleted” sample that is enriched in continuum events. The sideband, same-charge, and  $B\bar{B}$ -depleted samples serve as control samples for studying the  $\Delta t$  distributions of the backgrounds.

In the  $B^0 \rightarrow D^{*-}\rho^+$  analysis, about 11.5% of the partially reconstructed signal events are also fully reconstructed in the  $\bar{D}^0$  decay modes  $\bar{D}^0 \rightarrow K^+\pi^-$  or  $K^+\pi^-\pi^0$ . This yields a sample that, while relatively small, has a low background contamination of about 5%. This clean signal sample is used in the fits described below, improving the determination of the signal PDF parameters.

The  $B^0$  lifetime  $\tau_{B^0}$  is obtained in a three-step procedure using signal region and control sample events.

In the first step, the fractions  $f_i$  in the signal region and in the different control samples are obtained from kinematic-variable fits conducted simultaneously on the on- and off-resonance samples (and the fully reconstructed sample for the  $B^0 \rightarrow D^{*-}\rho^+$  signal region). The

fit PDF is that of Eq. (2), but with all  $\mathcal{F}_i(\Delta t, \sigma_{\Delta t})$  replaced by unity. In the  $B^0 \rightarrow D^{*-}\pi^+$  analysis this fit determines  $f_{\text{peak}}$  and  $f_{\text{cont}}$ . The fraction of  $B^0 \rightarrow D^{*-}\rho^+$  events  $f_{D^*X}$  in the  $B^0 \rightarrow D^{*-}\pi^+$  sample is assumed to be 16.8%, as predicted by the Monte Carlo simulation and the relative branching ratio [9]. This fit (Fig. 1(a)) yields  $6970 \pm 240$  signal  $B^0 \rightarrow D^{*-}\pi^+$  events. In the  $B^0 \rightarrow D^{*-}\rho^+$  analysis the kinematic-variable fit determines  $f_{\text{cont}}$ , as well as all the parameters of  $\mathcal{K}_{\text{cont}}(\xi)$ ,  $\mathcal{M}_{\text{sig}}(m_{\text{miss}})$ , and  $\mathcal{R}_{\text{sig}}(m(\pi^+\pi^0))$ . The parameters of  $\mathcal{D}_{\text{sig}}(F_\rho)$ ,  $\mathcal{K}_{\text{comb}}(\xi)$ , and  $\mathcal{K}_{\text{peak}}(\xi)$ , as well as  $f_{\text{peak}}/f_{\text{sig}}$  (9.7%) and  $f_{D^*a_1}/f_{\text{sig}}$  (11.6%), are obtained from the Monte Carlo simulation. The kinematic-variable fit to the  $B^0 \rightarrow D^{*-}\rho^+$  sample (Figs. 2(a), (b) and (c)) yields  $5520 \pm 250$   $B^0 \rightarrow D^{*-}\rho^+$  events, including  $691 \pm 36$  fully reconstructed events.

In the second step, all the parameters determined in the first step are fixed, and the parameters of  $\mathcal{F}_i(\Delta t, \sigma_{\Delta t})$  of the backgrounds are determined entirely from the control data samples. In the  $B^0 \rightarrow D^{*-}\pi^+$  case, the parameters of  $\mathcal{F}_{\text{cont}}(\Delta t, \sigma_{\Delta t})$  are obtained from a fit to the  $B\bar{B}$ -depleted sample, and those of the  $\mathcal{F}_{\text{comb}}(\Delta t, \sigma_{\Delta t})$  are obtained from the same-charge sample. The parameters of  $\mathcal{F}_{\text{peak}}(\Delta t, \sigma_{\Delta t})$  are assumed to be identical to  $\mathcal{F}_{\text{comb}}(\Delta t, \sigma_{\Delta t})$ . In  $B^0 \rightarrow D^{*-}\rho^+$ , the parameters of  $\mathcal{F}_{\text{comb}}(\Delta t, \sigma_{\Delta t})$  are determined from the sideband sample, and those of  $\mathcal{F}_{\text{peak}}(\Delta t, \sigma_{\Delta t})$  are obtained from the same-charge sample. Each of the  $B^0 \rightarrow D^{*-}\rho^+$  control sample fits is conducted simultaneously on the on- and off-resonance data, and the parameters of  $\mathcal{F}_{\text{cont}}(\Delta t, \sigma_{\Delta t})$  are determined for each control sample simultaneously with the  $B\bar{B}$  PDF parameters.

In the final step, using the background  $\mathcal{F}_i(\Delta t, \sigma_{\Delta t})$  parameters obtained in the previous step, the signal region sample is fit to extract the signal  $\mathcal{F}_{\text{sig}}(\Delta t, \sigma_{\Delta t})$  parameters. In  $B^0 \rightarrow D^{*-}\pi^+$  this fit has six free parameters describing  $\mathcal{F}_{\text{sig}}(\Delta t, \sigma_{\Delta t})$ . In  $B^0 \rightarrow D^{*-}\rho^+$ , the fit is done simultaneously to on- and off-resonance events, as well as fully reconstructed events, and has 15 free parameters describing  $\mathcal{F}_{\text{sig}}(\Delta t, \sigma_{\Delta t})$  and  $\mathcal{F}_{\text{cont}}(\Delta t, \sigma_{\Delta t})$ .

The results of the last fit step, shown in Figs. 1(b) and 2(d), are  $\tau_{B^0} = 1.510 \pm 0.040$  ps for  $B^0 \rightarrow D^{*-}\pi^+$  and  $\tau_{B^0} = 1.616 \pm 0.064$  ps for  $B^0 \rightarrow D^{*-}\rho^+$ , where the errors are statistical only. These results are obtained after a correction of  $-0.014 \pm 0.020$  ps ( $+0.071 \pm 0.028$  ps for  $B^0 \rightarrow D^{*-}\rho^+$ ), determined from the Monte Carlo simulation. The correction accounts for biases due to the fit procedure, the event selection and, in the  $B^0 \rightarrow D^{*-}\rho^+$  case, the effect of  $\bar{D}^0$  daughter tracks passing the cone cut and being used for the determination of the other  $B$  vertex. The errors in the corrections are propagated to the final result as systematic errors.

The systematic uncertainties are listed in Table I, and described here. (1) The fractions and the PDF parameters of the background components were varied by their statistical errors, taking into account mutual cor-

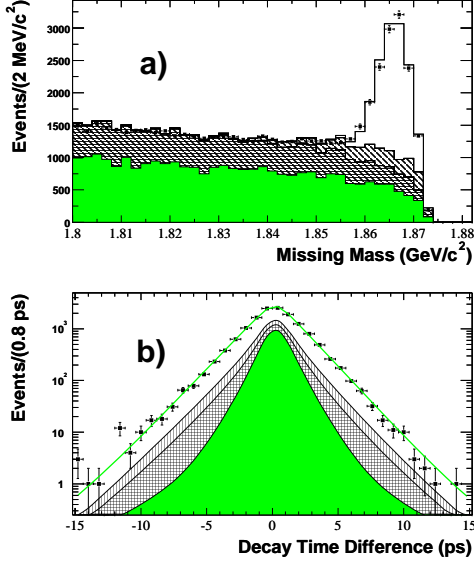


FIG. 1: Distributions of (a) missing mass and (b)  $\Delta t$  for candidate  $B^0 \rightarrow D^{*-}\pi^+$  events. The result of the fit (solid line) is superimposed on data (data points). The hatched, cross-hatched and shaded areas are the peaking  $B\bar{B}$ , combinatoric  $B\bar{B}$ , and continuum contributions, respectively. The  $\Delta t$  plot is obtained with the requirement  $m_{\text{miss}} > 1.860 \text{ GeV}/c^2$ .

relations, obtained from the fits of the first two analysis steps. (2) The PDF parameters and lifetime corrections that were obtained from the Monte Carlo simulation were varied by the statistical error in the Monte Carlo fits. The full analysis chain, including event reconstruction and selection, was tested with the Monte Carlo simulation, and the statistical precision of the consistency between the generated and fit lifetimes was assigned as a systematic error. The Monte Carlo statistical errors in the evaluation of the various corrections described above were propagated to the final result. (3) The level of  $B^0 \rightarrow D^{*-}\rho^+$  ( $B^0 \rightarrow D^{*-}a_1^+$ ) background in the  $B^0 \rightarrow D^{*-}\pi^+$  ( $B^0 \rightarrow D^{*-}\rho^+$ ) sample was varied by the relevant branching fraction errors [9], and the fraction of  $B \rightarrow D^{**}\rho^+$  background events in the  $B^0 \rightarrow D^{*-}\rho^+$  sample was varied between 0 and 40% of the signal yield. (4) The number of  $\bar{D}^0$  tracks satisfying the cone cut in the simulated sample was varied by  $\pm 5\%$  and the associated bias was reevaluated. (5) The parameters of  $\mathcal{F}_{\text{sig}}$  that were fixed in the fits were varied within conservative ranges. (6) Extensive parameterized Monte Carlo simulation studies were conducted to evaluate statistical biases in the fits due to limited data sample size or as the result of changes in the functional form of  $R((\Delta t - \Delta t_{\text{true}})/\sigma_{\Delta t})$ . (7) The  $\Delta t$  fit range was varied between  $|\Delta t| < 10$  ps and  $|\Delta t| < 20$  ps. (8) The  $z$  length scale of the detector has been determined with an uncertainty of 0.4% from the reconstruction of secondary interactions with a

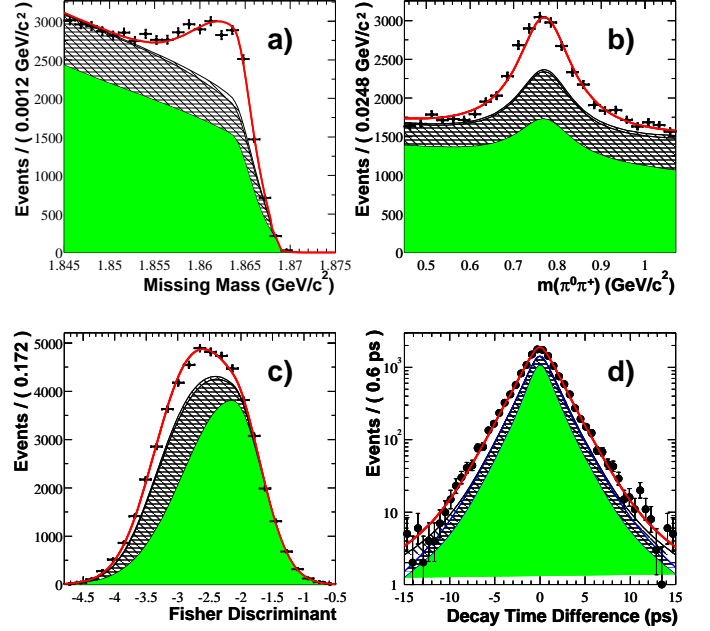


FIG. 2: Distributions of (a) missing mass, (b)  $\rho$  candidate invariant mass, (c) Fisher discriminant  $F_\rho$  and (d)  $\Delta t$  of  $B^0 \rightarrow D^{*-}\rho^+$  candidate events. The result of the fit (solid line) is superimposed on data (data points). The hatched, cross-hatched and shaded areas are the peaking  $B\bar{B}$ , combinatoric  $B\bar{B}$ , and continuum contributions, respectively. The  $\Delta t$  plot is obtained with the requirement  $m_{\text{miss}} > 1.854 \text{ GeV}/c^2$ ,  $0.60 < m(\pi^+\pi^0) < 0.93 \text{ GeV}/c^2$ , and  $F_\rho < -2.1$ .

TABLE I: Summary of the systematic uncertainties on the measured  $B^0$  lifetime.

Source	Errors (ps)	
	$B^0 \rightarrow D^{*-}\pi^+$	$B^0 \rightarrow D^{*-}\rho^+$
(1) Background parameters	0.023	0.044
(2) Monte Carlo statistics	0.021	0.042
(3) Fractional composition	0.008	0.024
(4) $D^0$ tracks bias	0.017	0.026
(5) $\Delta t$ resolution model	0.011	0.015
(6) Likelihood fit bias	0.005	0.016
(7) $\Delta t$ range	0.009	0.009
(8) $z$ scale	0.006	0.007
(9) SVT misalignment	0.008	0.008
(10) Beam energies	0.002	0.002
Total	0.041	0.075

beam pipe section of known length [15]. The systematic uncertainties related to the detector alignment (9) and beam energy uncertainty [8] (10) were also taken into account. The total systematic error in the  $B^0 \rightarrow D^{*-}\pi^+$  ( $B^0 \rightarrow D^{*-}\rho^+$ ) analysis is 0.041 ps (0.075 ps).

Several cross-checks were conducted to ensure the validity of the result. The data were fit in bins of the lab

frame polar angle, azimuthal angle, and momentum of the  $\pi_h$ , and in subsamples corresponding to different SVT alignment calibrations. The fit was repeated with different values of the cone cut ranging from 0.75 to 2.00 radians (0.6 to 1.2 radians for  $B^0 \rightarrow D^{*-}\rho^+$ ). Different functional forms of  $R((\Delta t - \Delta t_{\text{true}})/\sigma_{\Delta t})$  were used in the fit. In all cases, no statistically significant variation of the result was observed, beyond those already accounted for in the systematic errors.

In summary, in a sample of 22.7 million  $B\bar{B}$  pairs, we identify  $6970 \pm 240$   $B^0 \rightarrow D^{*-}\pi^+$  and  $5520 \pm 250$   $B^0 \rightarrow D^{*-}\rho^+$  partially reconstructed decays. These events are used to measure the  $B^0$  lifetime, obtaining  $\tau_{B^0} = 1.510 \pm 0.040$  (stat.)  $\pm 0.041$  (syst.) ps in  $B^0 \rightarrow D^{*-}\pi^+$  and  $\tau_{B^0} = 1.616 \pm 0.064$  (stat.)  $\pm 0.075$  (syst.) ps in  $B^0 \rightarrow D^{*-}\rho^+$ . The combined measurement, taking into account correlated errors, is

$$\tau_{B^0} = 1.533 \pm 0.034 \text{ (stat.)} \pm 0.038 \text{ (syst.) ps.}$$

This result is in good agreement with the world average  $B^0$  lifetime  $\tau_{B^0} = 1.542 \pm 0.016$  ps [9] and with other recent *BABAR* measurements [16], confirming the validity of using partially reconstructed events in time dependent measurements.

We are grateful for the excellent luminosity and machine conditions provided by our PEP-II colleagues, and for the substantial dedicated effort from the computing organizations that support *BABAR*. The collaborating institutions wish to thank SLAC for its support and kind hospitality. This work is supported by DOE and NSF (USA), NSERC (Canada), IHEP (China), CEA and CNRS-IN2P3 (France), BMBF and DFG (Germany), INFN (Italy), NFR (Norway), MIST (Russia), and PPARC (United Kingdom). Individuals have received support from the A. P. Sloan Foundation, Research Corporation, and Alexander von Humboldt Foundation.

<sup>†</sup> Also with Università della Basilicata, Potenza, Italy

- [1] Charge conjugate decays are implied.
- [2] R.G. Sachs, Enrico Fermi Institute Report, EFI-85-22 (1985) (unpublished); I. Dunietz and R.G. Sachs, Phys. Rev. D **37**, 3186 (1988) [E: Phys. Rev. D **39**, 3515 (1989)]; I. Dunietz, Phys. Lett. B **427**, 179 (1998); P.F. Harrison and H.R. Quinn (ed.), *BABAR* Physics Book, Chap. 7.6 (1998); D. London, N. Sinha, and R. Sinha, Phys. Rev. Lett. **85**, 1807 (2000).
- [3] N. Cabibbo, Phys. Rev. Lett. **10**, 531 (1963); M. Kobayashi and T. Maskawa, Prog. Theoret. Phys. **49**, 652 (1973).
- [4] The CLEO Collaboration, G. Brandenburg *et al.*, Phys. Rev. Lett. **80**, 2762 (1998).
- [5] The *BABAR* Collaboration, B. Aubert *et al.*, hep-ex/0203038, submitted to the XXXVII<sup>th</sup> Rencontres de Moriond on QCD and Hadronic Interactions, Les Arcs, France (2002).
- [6] The *BABAR* Collaboration, B. Aubert *et al.*, hep-ex/0203036, submitted to the XXXVII<sup>th</sup> Rencontres de Moriond on QCD and Hadronic Interactions, Les Arcs, France (2002).
- [7] “GEANT, Detector Description and Simulation Tool”, CERN program library long writeup W5013, 1994.
- [8] The *BABAR* Collaboration, B. Aubert *et al.*, Nucl. Instr. and Methods A **479**, 1 (2002).
- [9] The Particle Data Group, K. Hagiwara *et al.*, Phys. Rev. D **66**, 010001 (2002).
- [10] Unless explicitly noted, the value or procedure in the text refers to the  $B^0 \rightarrow D^{*-}\pi^+$  analysis while those in parentheses refer to the  $B^0 \rightarrow D^{*-}\rho^+$  analysis.
- [11] G. Fox and S. Wolfram, Phys. Rev. Lett. **41**, 1581 (1978).
- [12]  $\pi_h$  denotes both the charged pion from the  $\rho$  decay in  $B^0 \rightarrow D^{*-}\rho^+$  and the hard pion from  $B^0 \rightarrow D^{*-}\pi^+$ .
- [13] R. A. Fisher, Annals of Eugenics **7**, 179 (1936). M.S. Srivastava and E.M. Carter, “An Introduction to Applied Multivariate Statistics”, North Holland, Amsterdam (1983).
- [14] The ARGUS Collaboration, H. Albrecht *et al.*, Phys. Lett. B **254**, 288 (1991).
- [15] The *BABAR* Collaboration, B. Aubert *et al.*, Phys. Rev. D **66**, 032003 (2002).
- [16] The *BABAR* Collaboration, B. Aubert *et al.*, Phys. Rev. Lett. **87**, 201803 (2001); The *BABAR* Collaboration, B. Aubert *et al.*, Phys. Rev. Lett. **89**, 011802 (2002).

---

\* Also with Università di Perugia, Perugia, Italy